

Research on Dynamic Characteristics and Parameter Optimization of the Elastic Launch System of the Ruler Cannon

Wenjie Li^{1,a}, Biao Wang^{1,b,*}

¹University of Science and Technology Liaoning, Anshan, China

^a2982829567@qq.com, ^blxwyb@ustl.edu.cn

*Corresponding author

Abstract: The ruler cannon is a simple physics experiment device that converts elastic potential energy into kinetic energy. This paper adopts a core model consisting of two elastic rulers clamping a small ball, and systematically investigates the effects of factors such as applied force magnitude, ball mass, ruler angle, and force application position on the launch velocity of the ball, using nonlinear elasticity theory as well as the theorems of rigid-body translation and rotation. A complete set of motion equations, including normal force, friction, torque, and moment of inertia, is established through theoretical analysis. In the experiments, high-speed photography and trajectory methods are employed to measure the launch velocity and displacement of the ball. The results show that, due to its higher Young's modulus, a steel ruler stores elastic potential energy more efficiently than a plastic ruler. The launch velocity of the ball exhibits a non-monotonic variation with increasing external force. The farther the force application position is from the initial contact point of the ball, the higher the force transmission efficiency. As the ball mass increases, the launch velocity decreases. This study provides a theoretical basis and experimental support for the optimal design of elastic launch systems.

Keywords: elastic deformation; energy conversion; friction distribution; nonlinear elasticity

1. Introduction

As a common tool, the ruler possesses a slender structure that allows it to store elastic potential energy during bending. Upon release, this energy is converted into kinetic energy, producing a launching effect similar to a "cannon." This phenomenon is closely related to the energy transfer mechanisms in sports equipment such as golf clubs and tennis rackets, as well as engineering systems like electromagnetic catapults. This paper adopts a model consisting of two elastic rulers clamping a small ball. By combining nonlinear elasticity theory^[1] with the theorems of rigid-body translation and rotation^{[2][3]}, it analyzes the key parameters affecting the launch velocity of the ball. The theoretical model is validated through experiments, providing a reference for related fields.

2. Theoretical Model and Derivation

To establish a solvable physical model, the following reasonable assumptions are made: (1)Symmetry assumption: The system is symmetric about the line connecting the ball's center and the fulcrum. The deformation and forces on the upper and lower rulers are always identical;(2)Rigid ruler assumption (during motion analysis): During motion analysis, the rulers are assumed to be rigid rods. Their bending deformation is considered solely for storing and releasing energy and does not participate in the instantaneous force balance;(3)Contact point assumption: The ball remains in point contact with the rulers, and the contact points slide along the rulers;(4)Friction model: The sliding friction obeys Coulomb's law of friction^[4], and the friction coefficient μ is constant.

2.1. Geometric Relations

From symmetry, the center of the ball lies on the angle bisector of the two rulers. As shown in Figure 1, the geometric relationship satisfies:

$$\sin \frac{\theta}{2} = \frac{R}{b} \quad (1)$$

Therefore:

$$b = \frac{R}{\sin(\theta/2)} \quad (2)$$

$$d = b \cos \frac{\theta}{2} = R \cot \frac{\theta}{2} \quad (3)$$

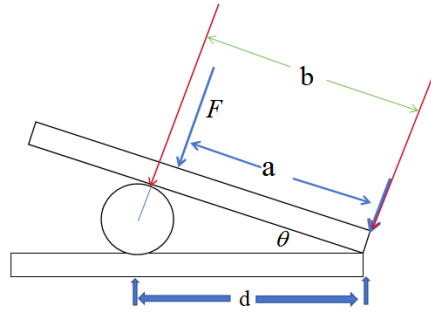


Figure 1: Ruler cannon model

2.2. Force Analysis

2.2.1. Calculation of Normal Force

When an external force F is applied perpendicular to the surface of the ruler at a distance a from the fulcrum, according to the lever principle, the equivalent pressure generated by this external force at the contact point is:

$$N_{\text{external force}} = \frac{a}{b} F \quad (4)$$

The direction of this pressure is perpendicular to the surface of the ruler and points toward the ball.

For the upper ruler, the normal force experienced by the ball is entirely generated by the transmission of the external force:

$$N_{\text{upper}} = \frac{a}{b} F \quad (5)$$

For the lower ruler:

$$N_{\text{lower}} = \frac{a}{b} F + mg \cos \frac{\theta}{2} \quad (6)$$

Since gravity only contributes additionally to the lower ruler, we have $N_{\text{lower}} > N_{\text{upper}}$. This is the fundamental reason for the rotation of the ball.

2.2.2. Calculation of Friction Force

According to Coulomb's law of friction, the magnitude of the sliding friction force is:

$$f_{\text{upper}} = \mu N_{\text{upper}} = \mu \frac{a}{b} F \quad (7)$$

$$f_{\text{lower}} = \mu N_{\text{lower}} = \mu \left(\frac{a}{b} F + mg \cos \frac{\theta}{2} \right) \quad (8)$$

2.3. Translational Motion Equation

2.3.1. Resultant Force in the Horizontal Direction

The resultant force acting on the ball in the horizontal direction (launch direction) includes the horizontal component of the normal force (driving) and the horizontal component of the friction force (opposing):

$$F_{Nx} = (N_{\text{upper}} + N_{\text{lower}}) \sin \frac{\theta}{2} \quad (9)$$

$$F_{fx} = (f_{\text{upper}} + f_{\text{lower}}) \cos \frac{\theta}{2} \quad (10)$$

Therefore, the resultant force in the horizontal direction is:

$$F_{\text{total}} = (N_{\text{upper}} + N_{\text{lower}}) \sin \frac{\theta}{2} - (f_{\text{upper}} + f_{\text{lower}}) \cos \frac{\theta}{2} \quad (11)$$

Substituting equations (5)–(8):

$$F_{\text{total}} = \left[\frac{a}{b} F + \left(\frac{a}{b} F + mg \cos \frac{\theta}{2} \right) \right] \sin \frac{\theta}{2} - (f_{\text{upper}} + f_{\text{lower}}) \cos \frac{\theta}{2} \quad (12)$$

Rearranging gives:

$$F_{\text{total}} = \left(2 \frac{a}{b} F + mg \cos \frac{\theta}{2} \right) \left(\sin \frac{\theta}{2} - \mu \cos \frac{\theta}{2} \right) \quad (13)$$

2.3.2. Work-Energy Relation and Velocity Solution

The work done by the external force F on the system is converted into: (1) the elastic potential energy stored in the rulers; (2) the work done against friction (internal energy); (3) the translational kinetic energy of the ball; (4) the rotational kinetic energy of the ball.

Let the displacement of the point of force application be δ [5][6] (the bending deflection of the ruler). The work done by the external force is:

$$W_F = F \cdot \delta \quad (14)$$

The elastic potential energy of the ruler (considering nonlinearity) is:

$$U_e = \int_0^{\delta} F(\delta) d\delta = \frac{1}{2} k \delta^2 + \text{higher-order terms} \quad (15)$$

where $k = \frac{3EI}{L^3}$ is the equivalent stiffness^[7], E is Young's modulus^[8], and I is the moment of inertia of the cross-section^[9].

The work done by friction is:

$$W_f = \int_{b_0}^{b_1} (f_{\text{upper}} + f_{\text{lower}}) ds \quad (16)$$

According to the work-energy theorem:

$$W_F - U_e - W_f = \frac{1}{2} mv^2 + \frac{1}{2} I \omega^2 \quad (17)$$

2.4. Rotational Effect Analysis

Since $N_{\text{lower}} > N_{\text{upper}}$, it follows that $f_{\text{lower}} > f_{\text{upper}}$. The magnitudes of the friction forces on the upper and lower sides are unequal, generating a resultant torque at the center of the ball.

The resultant torque acting on the ball is:

$$\tau = (f_{lower} - f_{upper})R \quad (18)$$

Substituting the expressions for the friction forces:

$$\tau = \mu \left[\left(\frac{a}{b} F + mg \cos \frac{\theta}{2} \right) - \frac{a}{b} F \right] R = \mu mg R \cos \frac{\theta}{2} \quad (19)$$

Important Conclusion: The resultant torque is independent of the external force F and is determined solely by gravity, the friction coefficient, the ball radius, and the angle between the rulers. This implies that even in the absence of an external force, the ball will acquire rotational motion when the rulers close under the influence of gravity alone.

The moment of inertia of the ball is:

$$I = \frac{2}{5} mR^2 \quad (20)$$

According to the rotational law $\tau = I\alpha$, the angular acceleration is:

$$\alpha = \frac{\tau}{I} = \frac{\mu mg \cos(\frac{\theta}{2})}{\frac{2}{5} mR^2} = \frac{5\mu \cos(\theta/2)}{2R} \quad (21)$$

The angular acceleration is independent of the ball's mass, inversely proportional to the radius R , and related to the angle θ . The smaller the ball radius, the more intense the rotation. Let the launch time be t , then the angular velocity is:

$$\omega = \alpha t \quad (22)$$

The rotational kinetic energy is:

$$E_{rot} = \frac{1}{2} I \omega^2 = \frac{1}{5} mR^2 \alpha^2 t^2 \quad (23)$$

After considering the rotational effect, the translational velocity of the ball is corrected as:

$$v = \sqrt{\frac{2(W_f - U_e - W_f) - I\omega^2}{m}} \quad (24)$$

2.5. Nonlinear Elastic Deformation

2.5.1. Nonlinear Deflection of the Ruler

Under large external forces, the relationship between the deflection of the actual ruler and the applied force deviates from linearity^[10]. According to nonlinear elasticity theory, the deflection can be expressed as:

$$\delta = \frac{F\alpha^3}{3EI} + \frac{\alpha F^2 \alpha^5}{5E^2 I^2} + \frac{\beta F^3 \alpha^7}{7E^3 I^3} \quad (25)$$

where α and β are nonlinear coefficients. The presence of the nonlinear term causes changes in the storage efficiency of elastic potential energy.

2.5.2. Contact Deformation of the Ball

Under pressure, the ball undergoes local deformation, and the contact area expands. According to Hertzian contact theory^[11], the contact radius c and the normal force N satisfy $c \propto N^{1/3}$. The increase in contact area leads to greater actual friction than that predicted by the point contact model, resulting in increased energy dissipation.

2.6. Summary of the Theoretical Model

Based on the above analysis, the launch velocity v of the ball is influenced by the following factors: (1) Geometric factors: The ball radius R determines the contact point position b and the angle θ . (2) External force factors: The magnitude of the external force F and its application position a affect the normal force and the storage of elastic potential energy. (3) Material factors: Young's modulus E of the ruler affects the elastic potential energy, while the friction coefficient μ affects energy dissipation. (4) Rotational effect: The difference in friction between the upper and lower sides causes the ball to rotate, consuming part of the energy. (5) Nonlinear effect: Nonlinear elasticity under large deformation reduces the efficiency of energy conversion.

The final expression for the launch velocity is:

$$v = \sqrt{\frac{2}{m}(W_f - U_e - W_f - \frac{1}{2}I\omega^2)} \tag{26}$$

3. Experimental Results and Data Analysis

In the experiments, weights were used to simulate the application of external force. High-speed photography and trajectory methods were employed to measure the launch velocity and displacement of the ball. Each set of experiments was repeated five times, and the average values were taken.

3.1. Effect of External Force Magnitude on Launch Velocity

The experimental data are shown in Table 1, and the corresponding velocity-external force relationship curve is shown in Figure 2.

As the applied force increases, the launch velocity of the ball exhibits a non-monotonic trend of first increasing, then decreasing, and then increasing again. In the initial stage, the increase in net force causes the velocity to rise. In the intermediate stage, the increase in frictional force leads to greater energy loss, causing the velocity to decrease. In the later stage, the friction approaches saturation, and the system releases the accumulated elastic potential energy, causing the velocity to rise again. The theoretical trend is generally consistent with the experimental trend, verifying the rationality of the model.

Table 1: Relationship between external force magnitude and launch velocity

External Force (N)	Experimental Velocity (m/s)	Theoretical Velocity (m/s)
1	4.11	4.64
2	7.60	10.37
3	3.10	3.28
5	5.16	5.68
6	6.19	7.32
10	10.31	13.45

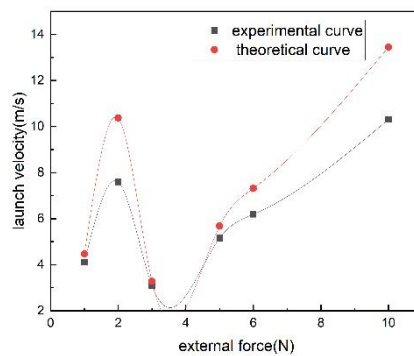


Figure 2: Velocity-external force relationship curve.

3.2. Effect of Ball Mass on Launch Velocity

The experimental data are shown in Table 2.

From Figure 3, the greater the mass of the ball, the smaller the launch velocity. An increase in mass leads to greater friction ($f = \mu N$, where N includes the gravitational component), resulting in increased energy loss. At the same time, inertia increases, causing a decrease in acceleration. The experimental results are consistent with the theoretical trend.

Table 2 Relationship between mass and launch velocity

mass (g)	Experimental Velocity (m/s)	Theoretical Velocity (m/s)
3	5.16	8.94
5	4.23	7.21
7	3.15	5.58
8	2.86	4.72
10	0.56	4.42

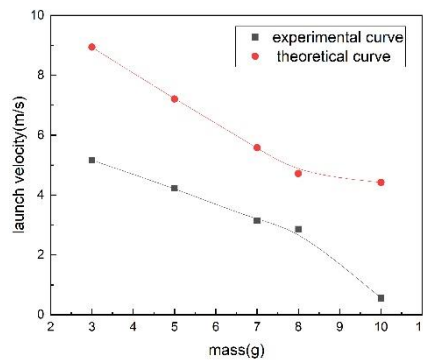


Figure3: Velocity-mass relationship curve.

3.3. Experiment on Ruler Material and Elastic Deformation

The experimental data are shown in Table 3.

Table 3 Relationship between ruler material and displacement distance

Ruler Material	Displacement Distance (cm)	Average Value (cm)
Plastic Ruler	43.6, 47.2, 45.5, 44.7, 46.2	45.6
Steel Ruler	99.3, 95.8, 92.9, 93.6, 91.6	95.6

The Young's modulus E of the steel ruler is much higher than that of the plastic ruler. According to Equation (25), the storage of elastic potential energy is more efficient, and the conversion to kinetic energy during release is more complete, resulting in a significant increase in displacement. This verifies the effect of material stiffness on the launching performance.

4. Conclusions

Through theoretical modeling and experimental investigation of the ruler cannon system, this paper draws the following conclusions: (1) Magnitude of external force: As the external force increases, the launch velocity exhibits a non-monotonic variation, which is related to friction saturation and the accumulation of elastic potential energy. (2) Ball mass: A larger ball mass leads to increased friction and inertia, resulting in a decrease in launch velocity. (3) Ruler material: The higher the Young's modulus, the more fully the elastic potential energy is stored, and the greater the launch velocity; the performance of the steel ruler is significantly superior to that of the plastic ruler.

Acknowledgements

I sincerely thank my supervisor, who showed me the direction and helped me navigate through the confusion, allowing me to continuously refine my research approach. This paper was supported by the College Student Innovation and Entrepreneurship Training Program of University of Science and Technology Liaoning (Grant No. X202510146201).

References

- [1] Fu Y B, Ogden R W. *Nonlinear elasticity: theory and applications. Journal of Elasticity* 82.3(2001):18-4.
- [2] Banerjee, Arun K., and John M. Dickens. "Dynamics of an arbitrary flexible body in large rotation and translation." *Journal of Guidance, Control, and Dynamics* 13.2 (1990): 221-227.
- [3] Favro, L. Dale. "Theory of the rotational Brownian motion of a free rigid body." *Physical Review* 119.1 (1960): 53.
- [4] Cross, Rod. "Coulomb's law for rolling friction." *American Journal of Physics* 84.3 (2016): 221-230.
- [5] Barten, H. J. "On the deflection of a cantilever beam." *Quarterly of Applied Mathematics* 2.2 (1944): 168-171.
- [6] Bisshopp, K. E., and Daniel C. Drucker. "Large deflection of cantilever beams." *Quarterly of applied mathematics* 3.3 (1945): 272-275.
- [7] Biancolini, M. E. "Evaluation of equivalent stiffness properties of corrugated board." *Composite structures* 69.3 (2005): 322-328.
- [8] Treacy, MM JEBBESSEN, Thomas W. Ebbesen, and John M. Gibson. "Exceptionally high Young's modulus observed for individual carbon nanotubes." *nature* 381.6584 (1996): 678-680.
- [9] Muir, P., K. A. Johnson, and M. D. Markel. "Area moment of inertia for comparison of implant cross-sectional geometry and bending stiffness." *Veterinary and comparative orthopaedics and traumatology* 8.03 (1995): 146-152.
- [10] Martin, R. Bruce, and David B. Burr. "Non-invasive measurement of long bone cross-sectional moment of inertia by photon absorptiometry." *Journal of biomechanics* 17.3 (1984): 195-201.
- [11] Fischer-Cripps, A. C. "The Hertzian contact surface." *Journal of materials science* 34.1 (1999): 129-137.